Polymer Testing 130 (2024) 108317

Contents lists available at ScienceDirect

Polymer Testing

journal homepage: www.elsevier.com/locate/polytest

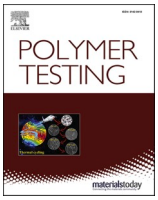

Bio and waste-based binders with hybrid rubberized-thermoplastic characteristics for roofing

Rodrigo Álvarez-Barajas, Antonio A. Cuadri, Clara Delgado-Sánchez, Francisco J. Navarro, Pedro Partal *

Pro²TecS-Chemical Process and Product Technology Research Centre, Department of Chemical Engineering, ETSI. Campus de "El Carmen", Universidad de Huelva, 21071, Huelva, Spain

ARTICLE INFO

Keywords:
Bio-based binders
Waste polymers
Crumb tyre rubber
Solar absorption

ABSTRACT

Non-bituminous binders with sustainable characteristics have been developed as potential roofing materials. A vegetable colophony rosin ester, waste cooking oil, waste crumb rubber and a blend of recycled high-density polyethylene (HDPE) and polypropylene (PP) have been used for binder formulations. Rheological, calorimetric and technological characterizations have been performed to assess the compatibility among binder components and optimal compositions. Additionally, thermal conductivity, heat capacity and solar radiation tests have been performed on selected non-bituminous and bitumen-based binders. Solar radiation experimental set-up has been simulated by Computational Fluid Dynamics (CFD) in order to get a deeper insight into heat transmission mechanisms involved. A binder formulation composed of 40 wt% maleic-modified rosin ester, 32 wt % waste oil, 20 wt% crumb rubber and 8 wt% recycled HDPE/PP blend has shown suitable mechanical properties and solar behaviour for roofing materials. The use of recycled thermoplastics and elastomers imparts material with a hybrid character, showing enhanced flexibility and softening points, respectively, at low and high in-service temperatures. Its solar behaviour is comparable to that of the modified bitumen, with a similar heat absorption from Sun (about 30 %) but lower heat storage capacity at ambient temperature.

1. Introduction

The greater global awareness about resource depletion and a more sustainable living manner have motivated the development of alternatives to traditional bituminous binders for roofing applications using waste and renewable resources [1,2]. Initially, the use of polymeric waste materials was found to enhance bitumen performance and sustainability [3,4]. Subsequently, as a natural step forward, researches aim for the development of non-bituminous binders formulated with recycled or bio-based feedstocks that cannot only help to enhance binder performance but also the transition into a circular economy and promote energy savings and environmental preservation [5–7]. Different approaches address the development of more environmentally friendly binders or bio-binders, given that the majority of formulations imply the use of waste materials and bio-oils of diverse origins as bitumen modifiers (around 10 % of total mix) [8–10],while others suggest their use as extenders (25 %–75 % replacement) [10,11].

Conversely, a limited number of publications and patents have successfully yielded non-bituminous or alternative binders [12,13]. Although some non-bituminous binders, usually referred to as synthetic binders, have been proposed in the past, they are mainly characterized by a non-bio-based nature [14,15]. Other alternative bio-based binders use mineral or fresh vegetable oils and wood byproducts mixed with diverse polymers exhibiting comparable physical properties and low temperature performance to those of a 50/70 conventional bitumen [16,17]. In this regard, the use of waste vegetable oil and the addition of high percentage of polymer wastes can be deemed valuable components for alternative binders in roofing materials, providing an environmental added value [18,19]. Furthermore, other works have shown that waste vegetable oil can provide impermeability and flexural strength when used as binder in the fabrication of roofing tiles [20,21].

In line with current sustainable demands, this research focuses on the design of novel bio-based non-bituminous binders, understand as a 100 % bitumen replacement, as potential roofing materials, which combine both wastes and bio-based components in their formulations. For this purpose, maleic-modified rosin ester from pine trees, waste cooking oil,

* Corresponding author.
E-mail address: partal@uhu.es (P. Partal).

https://doi.org/10.1016/j.polymertesting.2023.108317
Received 9 October 2023; Received in revised form 30 November 2023; Accepted 21 December 2023
Available online 22 December 2023

a mixture of recycled thermoplastics and crumb rubber from waste tyres have been used as raw materials.

Despite the high recyclability of polymers such as high-density polyethylene (HDPE) and polypropylene (PP), in most cases these thermoplastics end up being disposed in landfills, usually mixed with other plastics. As an alternative for such plastics blends, owing to their low toxicity and the lack of harmful gases emission in their melting process, they are safe to be used in binder formulations. Particularly, PP is one of the most widely used plastomers in roofing applications and HDPE has been also proposed for asphalt materials, as bitumen or non-bituminous binder modifiers due to their high melting point and excellent chemical and temperature resistance [12,22].

Unlike thermoplastics, the polymeric fraction of discarded tyres cannot be re-melted and is usually recovered as crumb rubber (CR) with selected ranges of particle size [23]. It is also widely used as bitumen modifier, being added to asphalt binders in proportions from 5 to 20 %, mainly to improve material behaviour at low in-service temperatures (i.e. by shifting its mechanical glassy region towards much lower temperatures). Interestingly, the combination of thermoplastics and CR has been found to improve the properties of modified bitumen binders at both low and high in-service temperatures [18,24–26]. Accordingly, the addition of the recycled PP/HDPE blend to the proposed non-bituminous binders is expected to impart roofing materials with high softening point and suitable stiffness at high in-service temperature, along with enhanced environmental resistance. Moreover, the combination of CR and PP/HDPE is expected to lead to a hybrid effect on mechanical material performance, by enhancing both its flexibility and dimensional stability, respectively at low and high temperatures.

Both polymeric modifiers will be dispersed in a continuous phase composed of vegetable waste oil and rosin ester, which have been selected considering their residual and renewal origins, respectively. Waste vegetable oil from cooking and frying activities is considered a serious environmental contaminant. Thus, different valorisation pathways have been proposed for this residue, such as biofuel production, bio-based plasticizes, surfactants, polymeric materials, rejuvenators of bituminous binders or bitumen replacement [1,27–29]. Investigations indicate that waste vegetable oil not only can improve low-temperature performance and fluidity of the binder blend [9,27] but when mixed with CR and PP/HPDPE could also enhance its rutting and fatigue resistance [30]. Furthermore, biomolecules present in waste vegetable oil could facilitate CR swelling in the binder and improve its thermal and UV aging [31,32].

Finally, numerous studies have proposed the use of rosin acids for the synthesis or modification of polymeric materials being considered as an inexpensive, bio-based, biodegradable and non-toxic raw material [33]. Rosin acids can provide hydrophobicity and improve thermo-physical, mechanical and functional properties of the final product [34]. Furthermore, they are expected to contribute to processability and performance of the binder enhancing the compatibility with the polymeric matrix [35,36].

As a result, this research focuses on the development of novel non-bituminous binders with improved sustainable characteristics as an alternative to traditional bituminous binders for roofing applications. To that end, this work addresses a comprehensive rheological, microstructural, and technological characterization of formulated non-bituminous binders, which helps understand the role of each component in the final material performance. Additionally, material thermal and solar behaviours have been assessed by conductivity, calorimetric and solar radiation tests conducted on a selected non-bituminous binder and compared with a reference SBS polymer-modified bitumen. The resulting binders may provide a greener and eco-friendlier alternative to traditional construction materials formulated with petroleum-derivatives.

2. Materials and methods

2.1. Materials and formulations

Binders were formulated with a rosin ester (R) supplied by Luresa, S.A. (Spain); recycled plastic (P) from Cordoplas S.A. (Spain); crumb rubber from discarded tyres (CR) supplied by RNC (Spain); and a waste vegetable cooking oil (O) mainly used for food frying supplied by BIOLIA, S.A (Spain). Rosin was a pentaerythritol ester of gum rosin modified by maleic anhydride with a melting point of 135 °C and 25 mg KOH/g acid number. Particle size of non-processed crumb rubber ranged between 0.5 and 2 mm. Recycled plastic was a blend of 65 wt% high density polyethylene (HDPE) and 35 wt% polypropylene (PP), being HDPE/PP ratio of 1.86. Binder formulations shown in Table 1 were prepared ranging R/O ratios from 0.75 to 1.5 and fixing polymers concentrations at 20 wt% CR and 8 wt% P. Additionally, two reference bituminous binder have been used for comparison: A) a neat bitumen B50/70 with 56 dmm penetration, 53.5 °C softening point and a SARAs composition of 4.8 % saturates, 52.3 % aromatics, 24.5 resins and 18.4 asphaltenes; and B) a SBS polymer modified bitumen with 75 °C softening point and 43 dmm penetration.

2.2. Binder processing and testing

Samples were prepared in a Silverson L5 Laboratory mixer, using a general-purpose disintegrating head, at 180 °C and 3800 rpm agitation speed for 120 min. Binder consistency was determined by penetration tests, stated by the European standard EN 1426, measuring the depth that a needle penetrates a sample of binder under the specified testing conditions (e.g. 25 °C). Material softening points (i.e. Ring-and-Ball softening temperatures) refer to the values at which a steel ball deforms the binder contained in a metal ring under the specified testing conditions stated in EN 1427.

Rheological characterization was conducted in a SmartPave 102e rheometer (Anton Paar, Austria), and consisted of frequency sweep tests in oscillatory shear and steady viscous flow measurements. Oscillatory frequency sweep tests, from 0.01 to 100 rad/s, were performed between −30 °C and 140 °C combining two plate-plate geometries (8 and 25 mm diameters with 2 mm and 1 mm gap, respectively). All oscillatory shear measurements were carried out at strains or stress values within the linear viscoelastic region (LVR). Viscous flow tests, between 0.1 and 100 s^{-1}, were carried using coaxial cylinder geometries at temperatures of 135, 165 and 180 °C.

Microstructural and thermal characterization involved Differential Scanning Calorimetry (DSC) analysis, carried out in a DSC TA Q100 and Q250 (TA Instruments, USA) from −80 °C to 180 °C using samples of 5–10 mg, placed into aluminium hermetic pans and 50 ml/min N_2 purge gas flow. Firstly, samples were heated above their melting points to avoid the effect of material past thermal history, after a controlled cooling, they were submitted to the main heating ramp at a rate of 10 °C/min. Material specific heat capacity was obtained by means of Modulated DSC, using 2 °C/min heating ramps and a temperature modulation of ±0.3 °C for 60 s.

Thermal conductivity tests, between 23 and 80 °C, were conducted in a THB 100 device from Linseis GmbH (Germany), using the Transient Hot-Bridge (THB) technique and a sensor type A with a metal frame (A-13890).

Solar irradiation tests were simulated by subjecting samples to a constant incident radiation power, using a Xenon lamp HXF300-T3 (Beijing China Education Au-light Technology Co., Ltd, China) with an attached filter AM 1.5G (300–1100 nm). A pyranometer SMP3 (Kipp & Zonnen, Netherlands) was used to measure the incident radiation. Testing specimens consisted of a binder disk (42 mm diameter and 8.5 mm thickness) with 5 temperature sensors located at different positions, four of them located at the centre (r = 0 mm) with readings at x = 0 mm (binder top surface), 2.23 mm, 3.37 mm and 6.80 mm depth. An

Table 1
Binder compositions and their penetration (Pen.) values and softening points ($T_{R\&B}$); viscoelastic activation energies (E_a) and zero-shear limiting viscosity (η_o); and DSC glass (T_g), melting (T_m) temperatures and melting enthalpies (ΔH_m).

Binder (R/O ratio)	R (%)	O (%)	CR (%)	P (%)	Pen.[1] (dmm)	$T^2_{R\&B}$ (°C)	E_a (kJ/mol)	η_o (Pa·s)	T_g (°C)	T_{m1} (°C)	ΔH_{m1} (J/g)	T_{m2} (°C)	ΔH_{m2} (J/g)
R/O = 0.75	31	41	20	8	125	67.7	–	–	−21.0	127.0	11.7	159.0	4.97
R/O = 1	36	36	20	8	87	105	–	–	−24.9	126.5	9.59	159.3	3.52
R/O = 1.125	38	34	20	8	44	132	145	$5.40\ 10^{10}$	−34.7	126.4	9.32	159.4	3.28
R/O = 1.25	40	32	20	8	33	125	151	$2.54\ 10^{11}$	−35.5	126.4	6.97	158.7	2.51
R/O = 1.5	43	29	20	8	28	129	157	$2.00\ 10^{10}$	−27.2	126.8	2.05	160.3	0.75

Tests conducted according to: (1) EN 1426 and (2) EN 1427.

additional temperature was recorded close to the sample wall (r = 20.925 mm and x = 2.36 mm). Sample side wall was isolated with a 77.6 mm-thickness insulator (k = 0.044 W/m °C, thermal conductivity), whereas its bottom side was in contact with isothermal heat sink, with selected cooling or sink temperatures of T_s = 32 and 37 °C. Experiential solar irradiation setup was simulated by Computational Fluid Dynamics (CFD) using Fluent-Ansys CFD 2020 software. An enclosure with dimensions 0.603x0.603 × 0.308 m (width-depth-height) that surrounds sample and insulator was created to simulate air motion due to natural convection (i.e. air buoyancy due to heat). A mesh containing approximately 470000 polyhedral cells was sufficient for this analysis, since the meshes with more elements led to similar results but involving an increased computational effort. Side and bottom walls of the enclosure were set as mass-flow inlets, whereas top wall was set as pressure outlet. Other main CFD settings were: a S2S radiation model with Solar Ray Tracing; a k-Epsilon viscous model; air density calculated by Boussinesq approach and conductivity changing with temperature according to a polynomial equation; and a Couple scheme selected as pressure-velocity coupling method.

3. Results and discussion

3.1. Material performance and microstructure

Polymer modified bitumen membranes are the most used roofing technique for low-slope roofs in the roofing market. For this type of products, non-bituminous binders should be characterized by high softening points and low penetration values. Table 1 shows that for a fixed polymer concentration (20 wt% CR and 8 wt% HDPE/PP), rosin addition increases material softening point from 67.7 to 132 °C and reduces penetration values from 125 to 28 dmm. However, softening points tend to a limiting value around 130 °C for R/O ratios above 1.125. Interestingly, for R/O ≥ 1.125 penetration and softening points match those established by the Spanish Standard UNE 104232-2 for modified bituminous mastics typically used in commercial roofing membranes, which demands a softening point higher than 110 °C and penetration values between 10 and 65 dmm. Additionally, concerning penetration and softening point values, these materials could be designed to match requirements established by ASTM D6152 (softening point between 85 and 116 °C and penetration between 20 and 60 dmm) for SBS-modified bitumen used in roofing.

Binder performance was also studied as a function of temperature by dynamic oscillatory shear tests. Fig. 1 shows material complex modulus (G*) obtained at 10 rad/s from −30 to 140 °C. It is worth noting that characteristics required for roofing material such as low-temperature flexibility and high-temperature structural integrity (e.g. compound or high thermal stability, vertical sag) are closely linked to material viscoelastic response. As expected, complex shear modulus decreases with increasing testing temperature. However, the slope of G* curves levels off between 20 and 120 °C (depending on the sample) and, subsequently, moduli drop suddenly above 120 °C. This limiting

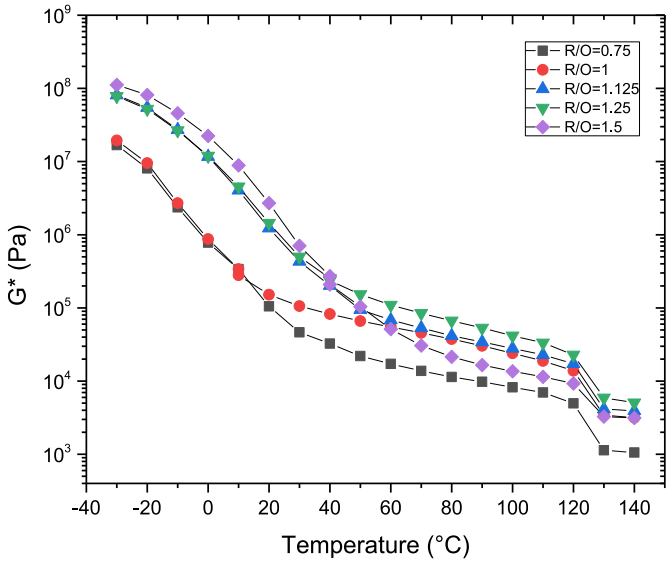

Fig. 1. Temperature dependence of binder complex modulus (G*) at 10 rad/s.

temperature would be related to the collapse of binder microstructure and, later, will be related to the melting process of the recycled plastic (i.e. HDPE/PP), swollen by some compounds of the oil/rosins blend. On the other hand, material exhibits a good low-temperature performance with complex modulus values that remain far below the viscoelastic glassy region, located at G*≈10^9 Pa, where material becomes brittle (i.e. showing lack of flexibility). As may be seen in Fig. 1, an increase in rosin concentration would reduce material flexibility at low temperatures, but always remaining below the glassy region. It is worth noting that rosin is brittle at temperatures below 70 °C but miscible with recycled oil, which shifts glass transition of the blend to lower temperatures (e.g. down to 10 °C for a R/O = 3) [37]. Thus, it is expected that material becomes stiffer, increasing binder complex modulus and glassy character, as rosin concentration is higher. Conversely, there is no apparent trend in the viscoelastic response at high temperature with the addition of rosin.

To shed some light on this issue, rheological time temperature superposition principle was applied, allowing us to study material viscoelasticity in a frequency range much wider than the experimental one. To that end, master curves of the elastic (G') and viscous (G") moduli, at a reference temperature of 30 °C, were obtained by means of a frequency shift factor, a_T, which leads to a reduced frequency, $\omega \cdot a_T$. As a result, both linear viscoelastic functions, in the range −30 to 110 °C (below material softening point), were empirically superposed onto master curves only for binders with R/O > 1.125 (Fig. 2). Although these materials are thermo-rheologically complex, empirical master curves for other complex bituminous and non-bituminous binders have been represented reasonably well elsewhere, providing useful information about the effects studied [38–41]. In any case, results obtained should only be

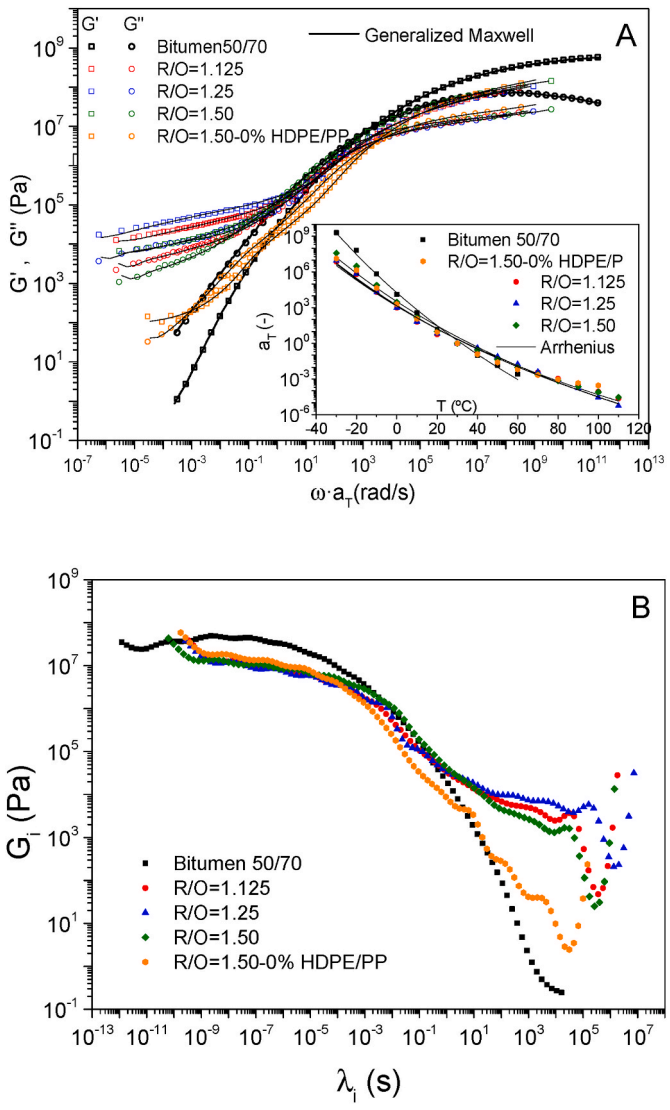

Fig. 2. A) Master curves, generalized Maxwell model fittings and shift factor dependence on temperature (inset) for bituminous and non-bituminous binders. B) Binder relaxation spectra calculated from Maxwell model.

qualitatively considered, just for comparison purposes.

Resultant empirical master curves of non-bituminous binders and a conventional 50/70 penetration neat bitumen are compared in Fig. 2A. Neat bitumen shows a continuous transition from the elastic (glassy) to the Newtonian region as frequency decreases. It is well-known bitumen compounds are of low molecular weight. Therefore, entanglement effects among molecules, related to the viscoelastic plateau region, are not expected [41,42]. Conversely a high molecular weight polymers-rich phase seems to be the responsible for the low frequency plateau region observed in non-bituminous binders, which contain recycled plastic and crumb rubber.

Moreover, the observed plateau region seems to be mainly related to the presence of HDPE/PP, as may be deduced from the mechanical response of the reference plastic-free binder formulated with 20 wt% CR and R/O = 1.5 (Fig. 2A). This binder exhibits a continuous decay of both moduli with decreasing frequency, being only visible the beginning of a plateau in G' at very low frequencies. A similar behaviour has been observed for crumb rubber modified bitumen above 20 wt% CR at high temperatures [43]. Under such conditions bitumen consistency is low enough to allow swollen rubber particles to control material viscoelasticity.

Inset of Fig. 2A shows temperature dependence of shift factors, a_T, used to obtain the master curves, which has been fitted to an Arrhenius-like equation, as follows:

$$a_T = exp\left[\frac{E_a}{R}\left(\frac{1}{T}-\frac{1}{T_o}\right)\right] \quad (1)$$

where T_o is the selected reference temperature, 30 °C (303.15 K), R the universal gas constant and E_a the viscoelastic activation energy. Table 1 shows that calculated activation energy values for non-bituminous binders were lower than that obtained for the reference bitumen (E_a = 212 kJ/mol), pointing out a lower thermal susceptibility for them [41,44,45]. However, the increase in R/O ratio seems to slightly increase E_a values.

A generalized Maxwell model may describe the observed dynamic linear viscoelastic behaviour of these systems:

$$G' = G_e + \sum_{i=1}^{N} G_i \frac{(\omega\lambda_i)^2}{1+(\omega\lambda_i)^2} \quad (2)$$

$$G'' = \sum_{i=1}^{N} G_i \frac{\omega\lambda_i}{1+(\omega\lambda_i)^2} \quad (3)$$

where G_e is the elastic modulus, λ_i the relaxation time, G_i relaxation strength and N the number of relaxation times. As a result, a characteristic spectrum of relaxation times was obtained for every binder (Fig. 2B). Binders containing HDPE/PP show two plateaus at low and intermediate relaxation times, unlike neat bitumen and reference non-bituminous binder (formulated without recycled plastic) that display only a plateau at low relaxation times. Thus, the first plateau, at low relaxation times, would be related to the resin/oil fraction. The second one would derive from the presence of plastic, likely swollen by the oil and/or rosin fractions, as will be seen later. Finally, the minimum observed at high relaxation times in all non-bituminous binders, formulated either with or without plastic, would be mainly attributed to the presence of swollen crumb rubber particles.

Furthermore, relaxation spectra were used to compare binder mechanical behaviour as a function of material composition. To that end, a characteristic material parameter, the low shear-limiting viscosity (η_o), was calculated as follows:

$$\eta_o = \sum_{i=1}^{N} G_i\lambda_i \quad (4)$$

where N = 90 was used for all the materials studied, which was optimized by the fitting software (RheoCompass). The resultant values of η_o for non-bituminous binders are shown in Table 1. Calculated viscosity value for neat bitumen (4.42 10^5 Pa s) is in good agreement with others previously published [40], and several orders of magnitude lower than those obtained for non-bituminous binders (Table 1). Among non-bituminous binders, system with R/O = 1.25 showed the highest value for this material parameter.

Finally, viscous behaviour of formulated binders, at temperatures related to their processing and laydown, is shown in Fig. 3. As may be seen in Fig. 3A, a non-Newtonian (shear thinning) behaviour was always found even at the highest tested temperature of 180 °C, with viscosity values decreasing with shear rate. All binders, no matter their formulations, present similar dependence (log-log slope) on shear rate, evidencing that the polymer-rich matrix controls binder rheology at this temperature. However, material viscosity (that decreases with temperature) increases as the rosin concentration (or R/O ratio) is higher (Fig. 3B). Among binders studied, systems R/O = 1.125 and R/O = 1.25 would balance low viscosity values at 180 °C, required for their manufacture, with suitable in-service mechanical properties (i.e. softening point, penetration and viscoelastic moduli). Additionally, their high viscosity at 135 °C would help pass dimensional stability tests at

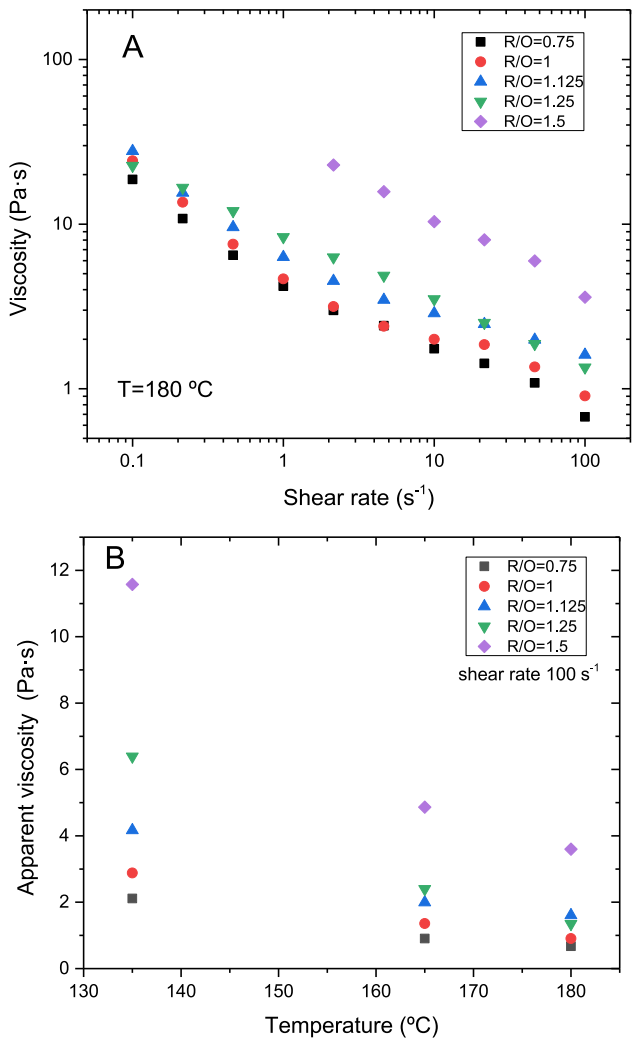

Fig. 3. Effect of rosin concentration on binder viscosity: A) flow curves at 180 °C; and B) apparent viscosity values at 100 s^{-1}.

elevated temperatures (e.g. UNE-EN 1107-1).

Blends performance depends directly on the compatibility between four components and sample microstructure that may be studied by means of DSC (Fig. 4). Pure recycled polymer presents two endothermic events with characteristic temperatures at 132.1 and 162.5 °C (Fig. 4A), which respectively correspond to HDPE and PP crystalline fraction melting processes [46]. Similarly, waste vegetable oil shows a crystalline fraction melting temperature of −17.6 °C, and an exothermic event located at −48 °C known as cold crystallization. Finally, rosin only shows a glass transition at around 73.8 °C, whereas crumb rubber shows no phenomena in the experimental temperature range (Fig. 4A).

After blending, oil cold crystallization/melting events are not visible and rosin glass transition is noticeably shifted to approximately −30 °C for all concentrations (Table 1), which has previously been related to a good compatibility between oil and rosin [37]. Given the high T_g = 73.8 °C of rosin, the glass transition of the R/O blend is expected to shift towards lower values as the oil concentration increases [47]. Conversely, thermodynamic T_g values shown in Table 1 tend to decrease as R/O is higher, with the lowest value (−35.5 °C) measured for the R/O = 1.25. In order to explain this issue, interactions between polymers and R/O blend need also to be considered.

On the other hand, in good agreement with results shown in Fig. 1, the sharp drop in G* observed at around 120 °C seems to be related to the first melting event located at c.a. 126 °C (Table 1), which corresponds to the HDPE melting (the most abundant polymer in the HDPE/PP blend). Thus, polymers melting temperatures drop about 5 °C for HDPE and between 2 and 4 °C for PP, suggesting polymers are being swollen by some compounds of the recycled oil/rosin blend, as previously found in polymer modified bitumens [48]. Likewise, their absorption by the polymer-rich phase may also hinder the formation of larger crystallites [49,50], which are known by their reinforcement effects on bituminous binders that enhance their rheological responses [51]. As shown in Table 1, a lower crystallinity is confirmed by the decrease of the melting enthalpies found for both polyolefins (HDPE and PP) present in these non-bituminous binders [37].

Initially, the presence of crystallites with smaller size would lead to lower viscoelastic moduli [37]. However, there are two opposite effects when R/O is raised, a hardening of rosin-oil blend leading to higher moduli [47], and a loss of crystallinity in the polymer-rich phase that reduces its contribution to the bulk viscoelastic response of the material at high in-service temperature. In this sense, binder formulated with R/O = 1.25, with the highest values of G* between 60 and 120 °C (Fig. 1), represents an optimum viscoelastic balance between both opposite effects.

As a result, the binder with R/O = 0.75 would have the highest crystallinity degree that decreases as R/O ratio is higher. Therefore, polymer would be swollen by the rosin-oil fraction, acting rosin as a compatibilizer, as suggested by Simon-Stőger and Varga [52] for other CR and HDPE systems compatibilized by maleic anhydride-based additives. Whereas binders with R/O $\leq$ 1 exhibit poor polymer compatibility (i.e. high crystallinity), binders with R/O $\geq$ 1.125 meet desired specifications (e.g. enhanced softening point, stiffness or flexibility at low temperature), and show lower thermodynamic glass transition temperatures derived from a polymer-rich phase with low crystallinity (Table 1), and the presence of CR whose swelling has been, likely, promoted by the waste vegetable oil used [31,32].

3.2. *Material behaviour under solar radiation*

Roofing materials under solar radiation behave according to their thermal properties (e.g., thermal conductivity, specific heat capacity, absorptivity, emissivity, etc.) and characteristics of the incoming radiation (e.g., wavelength, intensity, etc.) [53]. As previously stated, R/O ratios between 1.125 and 1.5 showed suitable thermo-mechanical properties to be used as roofing materials. Among them, for sake of comparison, system with R/O = 1.25 was selected for assessing its solar and thermal behaviours, and compared with a reference SBS polymer modified bitumen (characterized by 75 °C softening point and 43 dmm penetration).

Fig. 5A shows thermal conductivity (k) values of materials studied as a function of temperature. As may be seen, thermal conductivities hardly change within the experimental temperature range, showing modified bitumen a lower average value of 0.133 ± 0.001 W/m°C than the selected non-bituminous binder, k = 0.186 ± 0.002 W/m°C. On the contrary, heat capacity increases with temperature for both materials (Fig. 5B), presenting the non-bituminous binder lower values than bitumen at temperatures above −14 °C. Thus, compared with modified bitumen, it would be expected a lower heat storage capability (about 4 % lower) in roofing materials based on these non-bituminous binders.

Inset of Fig. 6A outlines solar irradiation setup used to apply different radiant flux densities, q*, on reference modified bitumen and binder R/O = 1.25. Fig. 6A also displays the typical patterns of recorded temperatures upon irradiation. They show a rapid increase of the top surface temperature, followed by the other temperatures, towards equilibrium temperatures that decrease as the distance from the top increases (Fig. 6A). These steady state temperatures will be used for calculations later.

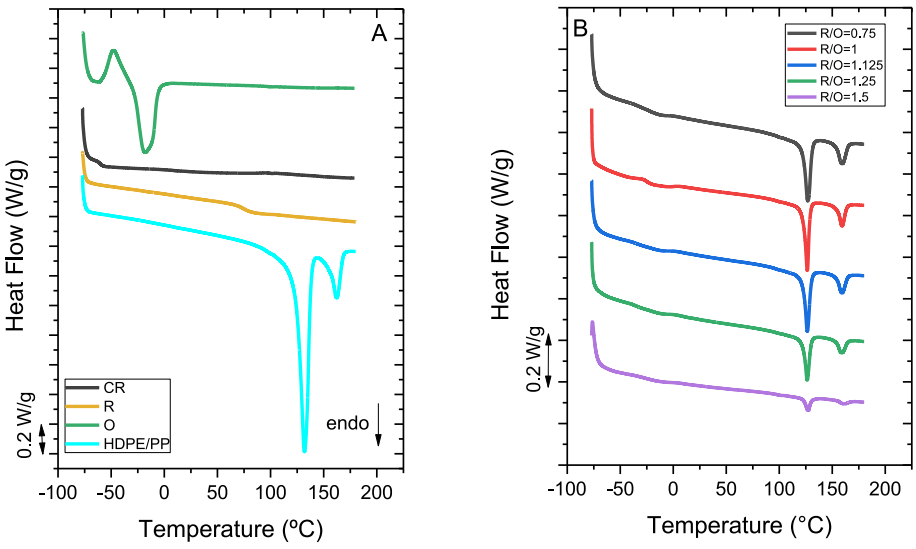

Fig. 4. DSC scans for pure components (A) and binders (B).

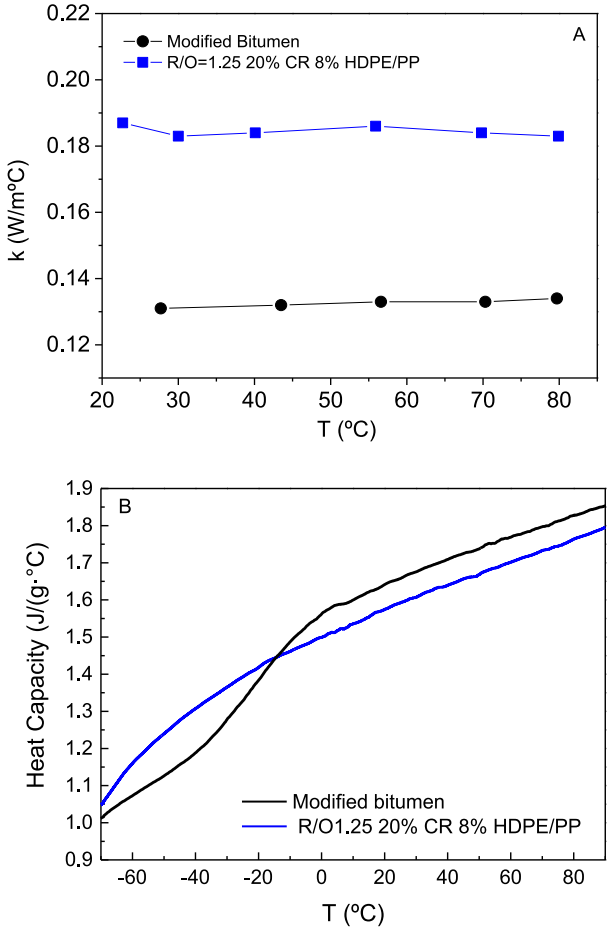

Fig. 5. Material thermal conductivity (A) and specific heat capacity (B) as a function of testing temperature.

Furthermore, with the aim of assessing the experimental setup and shedding some light on heat transmission mechanisms involved in solar experiments, CFD simulation were conducted on the reference modified

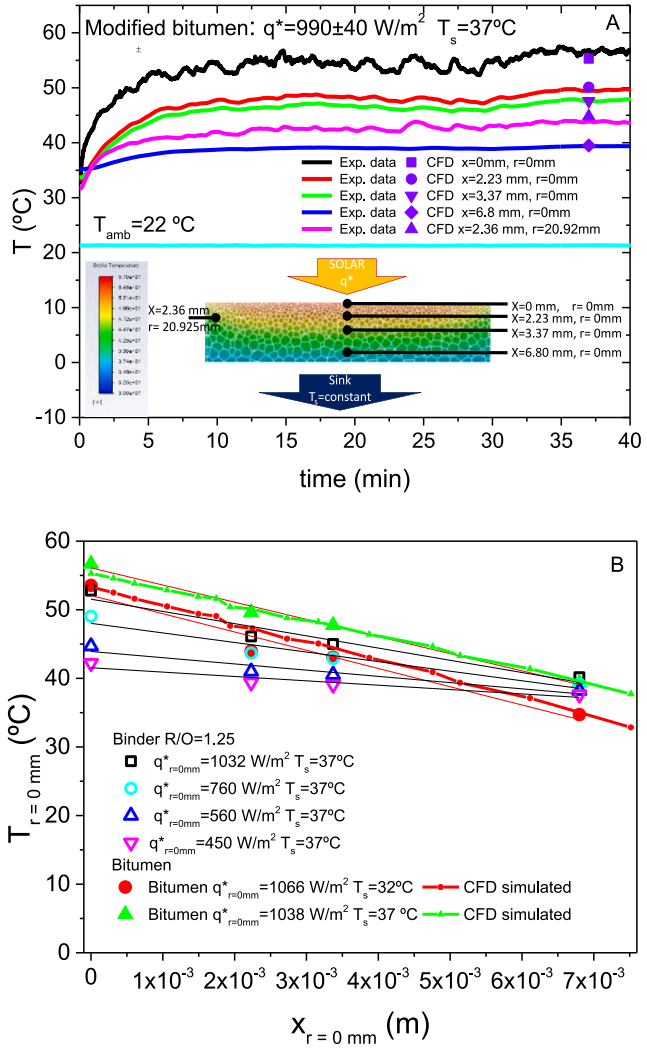

Fig. 6. A) Temperatures recorded at different sample positions (lines) with irradiation time and CFD-simulated steady state values (symbols). Inset: Experimental setup sketch and temperature CFD-simulated contours within the sample. B) Experimental and CFD-simulated temperatures along sample centre as a function of depth (x).

bitumen, as a well-known reference material (inset Fig. 6A). Selected conditions for CFD simulations on bitumen were an average solar irradiation of $q^*_{av} = 990 \pm 40$ W/m^2 (with a peak value at the sample centre, $q^*_{r\,=\,0mm} = 1066$ W/m^2), a sink temperature of $T_s = 37$ °C, and an experimental setup exposed to room conditions (air at $T_{amb} = 22$ °C). Simulation estimates an effective solar heat flux on sample top surface of 891 W/m^2 (in agreement with the bitumen albedo, 0.1), which is partially conducted through the top surface of the bituminous sample ($q_{cond} = 342$ W/m^2) and lost between binder and the environment due to thermal radiation ($q_{rad} = 203$ W/m^2) and convection (determined by difference as $q_C = 346$ W/m^2) mechanisms. Additionally, simulations estimate that about 29 % of heat conducted towards the sink is lost through the insulator. Finally, CFD simulation predicts fairly well experimental steady state temperatures recorded along the sample centre (Fig. 6A and B), and at the specimen wall (Fig. 6A).

Given the non-uniform temperature distribution inside the sample, for comparison purposes, temperatures recorded at the centre (r = 0 mm) may be used to calculate a local heat flux transferred due to a conduction mechanism, $q'_{cond(r\,=\,0mm)}$, by means of the Fourier's law:

$$q'_{cond\ (r=0mm)} = -k\frac{dT}{dx} \tag{5}$$

where k is the material thermal conductivity previously calculated, and x is related to the position of the recorded temperatures (Fig. 6).

Equation (5) leads to linear fits when applied to experimental data shown in Fig. 6B. This fact is due to thermal conductivity hardly depends on temperature (Fig. 5A). Therefore, fitting slopes (calculated as $-q'_{cond\ (r\,=\,0mm)}/k$) may be used to obtain the local heat flux conducted through sample (Fig. 7), and material solar heat absorption capability, q_{abs}, as follows:

$$q_{abs}(\%) = \frac{q'_{cond\ (r=0mm)}}{q^*_{r=0mm}} x100 \tag{6}$$

where $q^*_{r\,=\,0mm}$ is the applied solar irradiation flux at x = 0 and r = 0 mm. These values are also shown in Fig. 7 for comparison purposes.

As seen in Fig. 7, heat conducted through the sample would increase with Sun altitude or angle along the day, corresponding the lowest intensity $q^* = 450$ W/m^2 to $\alpha \approx 30°$ and the highest one $q^* = 1030$ W/m^2 to $\alpha \approx 80°$ [54]. However, under the selected experimental conditions ($T_s = 37$ °C and $T_{amb} = 23$ °C), heat absorbed (or conducted) by the non-bituminous binder (q_{abs}) remains close to 30 %, no matter the irradiation applied. This value is similar to that obtained for the reference modified bitumen when it is irradiated at $q^*_{r\,=\,0mm} = 1032$ and 1066 W/m^2, being sink temperatures, respectively, $T_s = 37$ °C and 32 °C (Fig. 7). Interestingly, these experimental results, calculated with local heat fluxes (i.e. temperatures recorded at r = 0 mm), are in good agreement with the average values predicated by CFD, despite the above commented non-uniform temperature distribution within the sample and calculated heat losses through insulator.

4. Conclusions

A bio-based rosin ester (R), a waste cooking oil (O), a waste crumb rubber (CR) and a recycled HDPE/PP blend (P) have been used in binder formulations with potential application in roofing. All samples showed a good low-temperature performance, with complex modulus far below the viscoelastic glassy region that increases with rosin concentration. Similarly, penetration and softening point values match the Spanish standard UNE 104232-2 for this type of materials.

Formulated binders have shown a plateau region at intermediate-high frequencies (or temperatures), which is mainly related to the presence of HDPE/PP. Additionally, crumb rubber controls binder viscoelasticity at high frequencies (or temperatures). Among non-bituminous binders, system with R/O = 1.25 showed enhanced viscoelastic properties in a wide range of temperatures and, therefore,

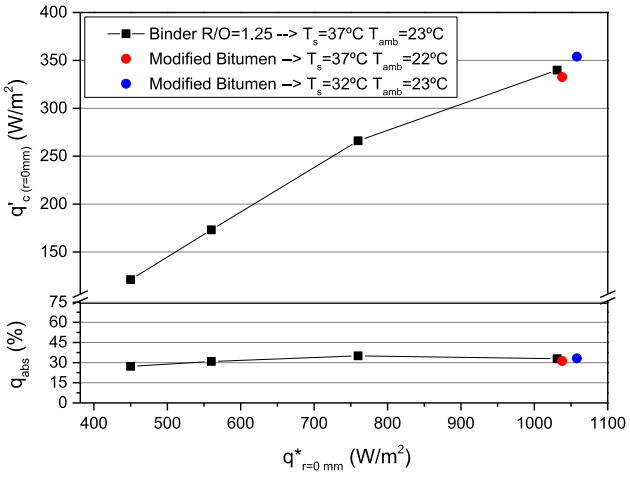

Fig. 7. Local heat flux conducted through the sample ($q'_{cond(r\,=\,0mm)}$) and material solar heat absorption capability (q_{abs}) as function of local irradiated heat flux ($q^*_{r\,=\,0mm}$).

improved in-service performance. Furthermore, this formulation has a low viscosity at 180 °C, required for its manufacture. Conversely, its high viscosity at 135 °C would help pass dimensional stability tests at elevated temperatures (e.g. UNE-EN 1107-1). Selected system showed about 4 % lower heat storage capacity and higher thermal conductivity than the reference bituminous binder. However, under solar radiation conditions, which mimic those typical of warm climates, the non-bituminous binder is expected to exhibit similar heat absorption capacity, around 30 %, to that of the reference polymer modified bitumen. Finally, it is worth noting that the practical use of these materials will depend on their response against long-term aging, processability, etc. Additionally, the final reduction in carbon emissions resulting from the production and use of these materials should be determined a comprehensive life cycle assessment.

CRediT authorship contribution statement

Rodrigo Álvarez-Barajas: Data curation, Formal analysis, Investigation, Writing – original draft. **Antonio A. Cuadri:** Data curation, Investigation, Methodology, Writing – review & editing. **Clara Delgado-Sánchez:** Data curation, Investigation, Methodology, Writing – review & editing. **Francisco J. Navarro:** Data curation, Investigation, Project administration. **Pedro Partal:** Conceptualization, Methodology, Project administration, Supervision, Writing – review & editing.

Declaration of competing interest

The authors declare that they have no known competing financial interests or personal relationships that could have appeared to influence the work reported in this paper.

Data availability

Data will be made available on request.

Acknowledgements

This work is co-funded by FEDER European Programme (80 %) and Junta de Andalucía (Consejería de Economía, Conocimiento, Empresas y Universidades/Agencia-IDEA) and of project TED2021-131284 B–I00 funded by MCIN/AEI/10.13039/501100011033 (Spanish Ministry of Science and Innovation) and European Union NextGenerationEU/PRTR. Clara Delgado-Sánchez also acknowledges financial support from Junta

de Andalucía through post-doctoral Grant No. DC 01228 (PAIDI 2020), co-funded by the EU Fondo Social Europeo (FSE).

References

[1] M.M.A. Aziz, T.M. Rahman, M. Hainin, W.A.W.A. Bakar, An overview on alternative binders for flexible pavement, Construct. Build. Mater. 84 (2015) 315–319, https://doi.org/10.1016/j.conbuildmat.2015.03.068.

[2] R. Mamat, M. Rosli Hanin, N.A. Hassan, N.A.R. Rahman, M.N.M. Warid, M. K. Idham, A review of performance asphalt mixtures bio-binder as alternative binder, J. Teknol. (Sci. Eng.) 77 (23) (2015) 17–20, https://doi.org/10.11113/jt.v77.6681.

[3] S. Wu, L. Montalvo, Repurposing waste plastics into cleaner asphalt pavement materials: a critical literature review, J. Clean. Prod. 280 (2021), 124355, https://doi.org/10.1016/j.jclepro.2020.124355.

[4] D. Nasr, R. Babagoli, M. Mazrouei, Evaluation of rheological behaviour of asphalt binder modified by recycled polyethylene wax and crumb rubber, Construct. Build. Mater. 328 (2022), 127069, https://doi.org/10.1016/j.conbuildmat.2022.127069.

[5] E. Fregonara, R. Giordano, D.G. Ferrando, S. Pattono, Economic-environmental indicators to support investment decisions: a focus on the buildings' end-of-life stage, Buildings 7 (3) (2017) 65, https://doi.org/10.3390/buildings7030065.

[6] M.R. Munaro, S.F. Tavares, L. Bragança, Towards circular and more sustainable buildings: a systematic literature review on the circular economy in the built environment, J. Clean. Prod. 260 (2020), 121134, https://doi.org/10.1016/j.jclepro.2020.121134.

[7] O.E. Ogunmakinde, T. Egbelakin, W. Sher, Contributions of the circular economy to the UN sustainable goals through sustainable construction, Resour. Conserv. Recycl. 178 (2022), 106023, https://doi.org/10.1016/j.resconrec.2021.106023.

[8] E.H. Fini, E.W. Kalberer, A. Shahbazi, M. Basti, Z. You, H. Ozer, HasanQ. Aurangzeb, Chemical characterization of biobinder from swine manure: sustainable modifier for asphalt binder, J. Mater. Civ. Eng. 23 (11) (2011) 1506–1513, https://doi.org/10.1061/(ASCE)MT.1943-5533.0000237.

[9] H. Wen, S. Bhusal, B. Wen, Laboratory evaluation of waste cooking oil-based bioasphalt as an alternative binder for Hot mix asphalt, J. Mater. Civ. Eng. 25 (10) (2013) 1432–1437, https://doi.org/10.1061/(ASCE)MT.1943-5533.0002941.

[10] M. Gong, J. Yang, J. Zhang, H. Zhu, T. Tong, Physical-chemical properties of aged asphalt rejuvenated by bio-oil derived from biodiesel residue, Construct. Build. Mater. 105 (2016) 35–45, https://doi.org/10.1016/j.conbuildmat.2015.12.025.

[11] X. Yang, Z. You, J. Mills-Beale, Asphalt binders blended with a high percentage of biobinders: aging mechanism using FTIR and rheology, J. Mater. Civ. Eng. 27 (4) (2015), 04014157, https://doi.org/10.1061/(ASCE)MT.1943-5533.0001117.

[12] M.A. Raouf, R.C. Williams, Temperature and shear susceptibility of a nonpetroleum binder as a pavement, Material. Transport. Res. Rec. 2180 (1) (2010) 9–18, https://doi.org/10.3141/2180-02.

[13] Z. Zhang, Y. Fang, J. Yang, X. Li, A comprehensive review of bio-oil, bio-binder and bio-asphalt materials: they source, composition preparation and performance, J. Traffic Transport. Eng. 9 (2) (2022) 151–156, https://doi.org/10.1016/j.jtte.2022.01.003.

[14] G.D. Airey, M.H. Mohammed, C. Fichter, Rheological characteristics of synthetic road binders, Fuel 87 (2008) 1763–1775, https://doi.org/10.1016/j.fuel.2008.01.012.

[15] C. Fuentes-Audén, F.J. Martínez-Boza, F.J. Navarro, P. Partal, C. Gallegos, Formulation of new synthetic binders: thermo-mechanical properties of recycledpolymer/oil blends, Polym. Test. 26 (2007) 323–332, https://doi.org/10.1016/j.polymertesting.2006.11.002.

[16] S. Pouget, F. Loup, Thermo-mechanical behaviour of mixtures containing bio-binders, Road Mater. Pavement Des. 14 (1) (2013) 212–226, https://doi.org/10.1080/14680629.2013.774758.

[17] E. Chailleux, M. Audo, S. Goyer, C. Queffelec, O. Marzouk, 11 - advances in the development of alternative binders from biomass for the production of biosourced road binders, in: S.C. Huang, H. Di Benedetto (Eds.), Woodhead Publishing Series in Civil and Structural Engineering, Advances in Asphalt Materials, Woodhead Publishing, 2015, pp. 347–362, https://doi.org/10.1016/B978-0-08-100269-8.00011-8.

[18] F.J. Navarro, P. Partal, F.J. Martínez-Boza, C. Gallegos, Novel recycled polyethylene/ground tire rubber/bitumen blends for use in roofing applications: thermo-mechanical properties, Polym. Test. 29 (2010) 1–8, https://doi.org/10.1016/j.polymertesting.2010.03.010.

[19] H. Wang, P. Rath, W.G. Buttlar, Recycled asphalt shingle modified asphalt mixture design and performance evaluation, J. Traffic Transport. Eng. 7 (2) (2020) 205–214, https://doi.org/10.1016/j.jtte.2019.09.004.

[20] H. Nadeen, N.Z. Habib, C.A. Ng, S.E. Zoorob, Z. Mustaffa, S.Y. Chee, M. Younas, Utilization of catalyzed waste vegetable oil as a binder for the production of environmentally friendly roofing tiles, J. Clean. Prod. 145 (2017) 250–261, https://doi.org/10.1016/j.jclepro.2017.01.028.

[21] S.S. Sam, N.Z. Habib, N.C. Aun, C.S. Yong, M.J.K. Bashir, T.W. Ping, Blended waste oil as alternative binder for the production of environmental friendly roofing tiles, J. Clean. Prod. 258 (2020), 120937, https://doi.org/10.1016/j.jclepro.2020.120937.

[22] E.S. Okhotnikova, Y.M. Ganeeva, I.N. Frolov, T.N. Yusupova, G.R. Fazylzyanova, Structural characterization and application of bitumen modified by recycled polyethylenes, Construct. Build. Mater. 316 (2022), 126118, https://doi.org/10.1016/j.conbuildmat.2021.126118.

[23] K. Formela, Waste tyre rubber-based materials: processing, performance properties and development strategies, Adv. Ind. Eng. Polym. Res. 5 (4) (2022) 234–247, https://doi.org/10.1016/j.aiepr.2022.06.003.

[24] L. Brasileiro, F. Moreno-Navarro, R. Tauste-Martínez, J. Matos, M.C. Rubio-Gámez, Reclaimed polymers as asphalt binder modifiers for more sustainable roads: a review, Sustainability 11 (3) (2019) 646, https://doi.org/10.3390/su11030646.

[25] M. Sol-Sánchez, A. Jiménez del Barco Carrión, A. Hidalgo-Arroyo, F. Moreno-Navarro, L. Saiz, M.C. Rubio-Gámez, Viability of producing sustainable asphalt mixtures with crumb rubber bitumen at reduced temperatures, Construct. Build. Mater. 265 (2020), 120154, https://doi.org/10.1016/j.conbuildmat.2020.120154.

[26] G.M. Duarte, A.L. Faxina, High-temperature rheological properties of asphalt binders modified with recycled low-density polyethylene and crumb rubber, Construct. Build. Mater. 298 (2021), 123852, https://doi.org/10.1016/j.conbuildmat.2021.123852.

[27] H.H. Joni, R.H.A. Al-Rubaee, M.A. Al-Zerkani, Characteristics of asphalt binder modified with waste vegetable oil and waste plastics, IOP Conf. Ser. Mater. Sci. Eng. 737 (1) (2020), 012126, https://doi.org/10.1088/1757-899X/737/1/012126.

[28] R.B. Ahmed, K. Hossain, Waste cooking oil as an asphalt rejuvenator: a state-of-the-art review, Construct. Build. Mater. 230 (2020), 116985, https://doi.org/10.1016/j.conbuildmat.2019.116985.

[29] F.F. de Albuquerque Landi, C. Fabiani, B. Castellani, F. Cotana, A.L. Pisello, Environmental assessment of four waste cooking oil valorization pathways, Waste Manag. 138 (2022) 219–233, https://doi.org/10.1016/j.wasman.2021.11.037.

[30] Z. Elahi, F. Mohd Jakarni, R. Muniandy, S. Hassim, M.S. Ab Razak, A.H. Ansari, M. M. Ben Zair, Waste cooking oil as a sustainable bio modifier for asphalt modification: a review, Sustainability 13 (2021), 11506, https://doi.org/10.3390/su132011506.

[31] S.F. Kabir, M. Mousavi, E.H. Fini, Selective adsorption of bio-oils' molecules onto rubber surface and its effects on stability of rubberized asphalt, J. Clean. Prod. 252 (2020), 119856, https://doi.org/10.1016/j.jclepro.2019.119856.

[32] L. Lyu, J. Pei, N.A. Burnham, E.H. Fini, L.D. Poulikakos, Nanoscale Evolution of rubber-oil modified asphalt binder after thermal and UV aging, J. Clean. Prod. 426 (2023), 13098, https://doi.org/10.1016/j.jclepro.2023.139098.

[33] L. Vevere, A. Fridrihsone, M. Kirpluks, U. Cabulis, A review of wood biomass-based fatty acids and rosin acids use in polymeric materials, Polymers 12 (11) (2020) 2706, https://doi.org/10.3390/polym12112706.

[34] K. Yao, J. Wang, W. Zhang, J.S. Lee, C. Wang, F. Chu, X. He, C. Tang, Degradable rosin-ester – caprolactone graft copolymers, Biomacromolecules 12 (6) (2011) 2171–2177, https://doi.org/10.1021/bm200460u.

[35] S. Kugler, P. Ossowicz, K. Malarczyzyk-Matusiak, E. Wierzbicka, Advances in rosin-based chemicals: the latest recipes, applications and future trends, Molecules 24 (9) (2019) 1651, https://doi.org/10.3390/molecules24091651.

[36] M. Aldas, C. Pavon, J. López-Martínez, M.P. Arrieta, Pine resin derivatives as sustainable additives to improve the mechanical and thermal properties of injected moulded thermoplastic starch, Appl. Sci. 10 (7) (2020) 2561, https://doi.org/10.3390/app10072561.

[37] R. Álvarez–Barajas, A.A. Cuadri, C. Delgado-Sánchez, F.J. Navarro, P. Partal, Non-bituminous binders formulated with bio-based and recycled materials for energy-efficient roofing applications, J. Clean. Prod. 393 (2023), 136350, https://doi.org/10.1016/j.jclepro.2023.136350.

[38] L. Zanzotto, J. Stasna, O. Vacin, Thermomechanical properties of several polymer modified asphalts, Appl. Rheol. 10 (3) (2000) 185–191, https://doi.org/10.1515/arh-2000-0012.

[39] A.A. Yousefi, A. Ait-Kadi, C. Roy, Effect of used-tire-derived pyrolytic oil residue on the properties of polymer-modified asphalts, Fuel 79 (8) (2000) 975–986, https://doi.org/10.1016/S0016-2361(99)00216-1.

[40] F.J. Navarro, P. Partal, F. Martínez-Boza, C. Gallegos, Thermo-rheological behaviour and storage stability of ground tire rubber-modified bitumens, Fuel 83 (2004) 2041–2049, https://doi.org/10.1016/j.fuel.2004.04.003, 14-15.

[41] F.J. Navarro, P. Partal, F. Martínez-Boza, C. Gallegos, Effect of composition and processing on the linear viscoelasticity of synthetic binders, Eur. Polym. J. 41 (6) (2005) 1429–1438, https://doi.org/10.1016/j.eurpolymj.2004.12.006.

[42] X. Lu, U. Isacsson, Rheological characterization of styrene-butadiene-styrene copolymer modified bitumens, Construct. Build. Mater. 11 (1) (1997) 23–32, https://doi.org/10.1016/S0950-0618(96)00033-5.

[43] F.J. Navarro, P. Partal, F. Martínez-Boza, C. Gallegos, Influence of crumb rubber concentration on the rheological behavior of a crumb rubber modified bitumen, Energy Fuels 19 (5) (2005) 1984–1990, https://doi.org/10.1021/ef049699a.

[44] P. Partal, F. Martinez-Boza, B. Conde, C. Gallegos, Rheological characterization of synthetic binders and unmodified bitumens, Fuel 78 (1) (1999) 1–10, https://doi.org/10.1016/S0016-2361(98)00121-5.

[45] A. Ait-Kadi, B. Brahimi, M. Bousmina, Polymer blends for enhanced asphalt binders, Polym. Eng. Sci. 36 (12) (1996) 1724–1733, https://doi.org/10.1002/pen.10568.

[46] H.J. Lin, Y.J. Pan, C.F. Liu, C.L. Huang, C.T. Hsieh, C.K. Chen, Z.I. Lin, C.W. Lou, Preparation and compatibility evaluation of polypropylene/high density polyethylene polyblends, Materials 8 (12) (2015) 8850–8859, https://doi.org/10.3390/ma8125496.

[47] C. Fuentes-Audén, F. Martínez-Boza, F.J. Navarro, P. Partal, C. Gallegos, Viscous flow properties and phase behaviour of oil–resin blends, Fluid Phase Equil. 237 (2005) 117–122, https://doi.org/10.1016/j.fluid.2005.08.017.

[48] J.C. Munera, E.A. Ossa, Polymer modified bitumen: optimization and selection, Mater. Des. 62 (2014) 91–97, https://doi.org/10.1016/j.matdes.2014.05.009.

[49] A.H. Fawcett, T. McNally, G.M. McNally, F. Andrews, J. Clarke, Blends of bitumen with polyethylenes, Polymer 40 (23) (1999) 6337–6349, https://doi.org/10.1016/S0032-3861(98)00779-4.
[50] A.H. Fawcett, T. McNally, Blends of bitumen with various polyolefins, Polymer 41 (14) (2000) 5315–5326, https://doi.org/10.1016/S0032-3861(99)00733-8.
[51] A. Yuliestyan, A.A. Cuadri, M. García-Morales, P. Partal, Influence of polymer melting point and Melt Flow Index on the performance of ethylene-vinyl-acetate modified bitumen for reduced-temperature application, Mater. Des. 96 (2016) 180–188, https://doi.org/10.1016/j.matdes.2016.02.003.
[52] L. Simon-Stőger, Cs Varga, PE-contaminated industrial waste ground tire rubber: how to transform a handicapped resource to a valuable one, Waste Manag. 119 (2021) 111–121, https://doi.org/10.1016/j.wasman.2020.09.037.
[53] S.R.O. Aletba, N.A. Hassan, R.P. Jaya, E. Aminudin, M.Z.H. Mahmud, A. Mohamed, A.A. Hussein, Thermal performance of cooling strategies for asphalt pavement: a state-of-the-art review, J. Traffic Transport. Eng. 8 (3) (2021) 356–373, https://doi.org/10.1016/j.jtte.2021.02.001.
[54] J.P. Holman, Heat Transfer, eight edition, McGraw-Hill Inc, New York, 1997.